HHS Public Access

Author manuscript

Prog Neurobiol. Author manuscript; available in PMC 2023 September 01.

Published in final edited form as:

Prog Neurobiol. 2023 August ; 227: 102482. doi:10.1016/j.pneurobio.2023.102482.

Intracellular accumulation of tau oligomers in astrocytes and their synaptotoxic action rely on Amyloid Precursor Protein Intracellular Domain-dependent expression of Glypican-4

Giulia Puliatti[a,*], **Domenica Donatella Li Puma**[a,b,*], **Giuseppe Aceto**[a,b], **Giacomo Lazzarino**[c], **Erica Acquarone**[d], **Renata Mangione**[e], **Luciano D'Adamio**[f], **Cristian Ripoli**[a,b], **Ottavio Arancio**[d], **Roberto Piacentini**[a,b,#], **Claudio Grassi**[a,b]

[a.]Department of Neuroscience, Università Cattolica del Sacro Cuore, Largo F. Vito 1, 00168, Rome, Italy

[b.]Fondazione Policlinico Universitario A. Gemelli IRCCS, Largo A. Gemelli 8, Rome, Italy

[c.]UniCamillus - Saint Camillus International University of Health Sciences, Via di Sant'Alessandro 8, Rome, 00131, Italy

[d.]Taub Institute, Department of Pathology and Cell Biology, and Department of Medicine, Columbia University, 630W 168th Street, New York, NY 10032, USA

[e.]Department of Basic biotechnological sciences, intensivological and perioperative clinics, Università Cattolica del Sacro Cuore, Largo F. Vito 1, 00168, Rome, Italy

[f.]Institute of Brain Health, Rutgers New Jersey Medical School, 205 South Orange Ave, Newark, NJ 07103, USA

Abstract

Several studies including ours reported the detrimental effects of extracellular tau oligomers (ex-oTau) on glutamatergic synaptic transmission and plasticity. Astrocytes greatly internalize ex-oTau whose intracellular accumulation alters neuro/gliotransmitter handling thereby negatively affecting synaptic function. Both amyloid precursor protein (APP) and heparan sulfate proteoglycans (HSPGs) are required for oTau internalization in astrocytes but the molecular mechanisms underlying this phenomenon have not been clearly identified yet.

Here we found that a specific antibody anti-glypican 4 (GPC4), a receptor belonging to the HSPG family, significantly reduced oTau uploading from astrocytes and prevented oTau-induced alterations of Ca^{2+}-dependent gliotransmitter release. As such, anti-GPC4 spared neurons co-cultured with astrocytes from the astrocyte-mediated synaptotoxic action of ex-oTau, thus preserving synaptic vesicular release, synaptic protein expression and hippocampal LTP at CA3-

[#]**Corresponding author**: Roberto Piacentini, Department of Neuroscience, Università Cattolica del Sacro Cuore, Largo F. Vito 1, 00168, Roma, Italy. roberto.piacentini@unicatt.it.

[*]These authors equally contributed to this work

CA1 synapses. Of note, the expression of GPC4 depended on APP and, in particular, on its C-terminal domain, AICD, that we found to bind *Gpc4* promoter. Accordingly, GPC4 expression was significantly reduced in mice in which either APP was knocked-out or it contained the non-phosphorylatable amino acid alanine replacing threonine 688, thus becoming unable to produce AICD. Collectively, our data indicate that GPC4 expression is APP/AICD-dependent, it mediates oTau accumulation in astrocytes and the resulting synaptotoxic effects.

Graphical Abstract

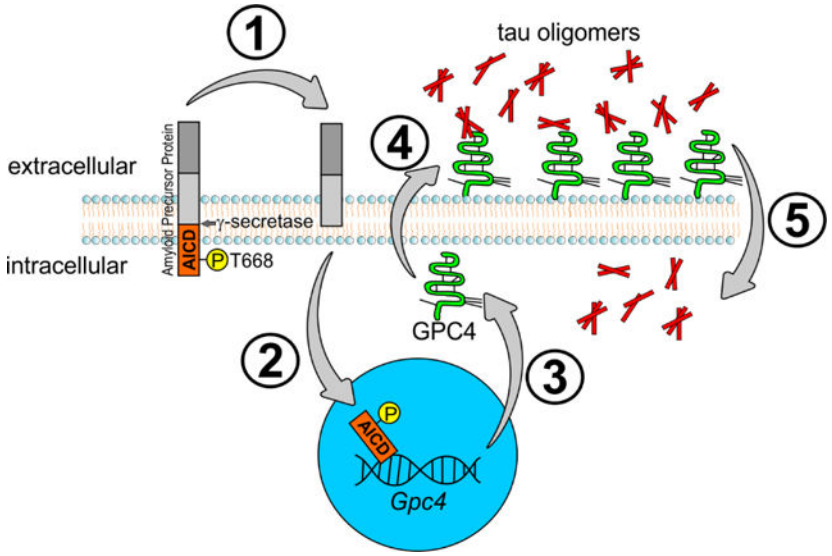

Keywords

tau oligomers; astrocytes; glypican 4; synaptic plasticity; AICD

Background

In the last years, several studies including ours demonstrated that extracellular (ex) tau oligomers (oTau) exert a strong detrimental action on synaptic function, thus contributing to the pathogenesis of several neurological illnesses, including Alzheimer's disease (AD) and other tauopathies. Indeed, in mouse models of these diseases oTau impair hippocampal synaptic transmission, long-term potentiation (LTP) at CA3-CA1 synapse and memory (Fá et al., 2016; Li Puma et al., 2022; Marcatti et al., 2022; Piacentini et al., 2017; Puzzo et al., 2017; Siano et al., 2021). Moreover, positron emission tomography studies carried out on humans demonstrated a strong correlation between tau accumulation in various brain areas (e.g., enthorinal cortex, inferior parietal cortex, frontal and anterior temporal cortices, etc.) and cognitive decline (Aschenbrenner et al., 2018; Lagarde et al., 2022; Mecca et al., 2022; Pontecorvo et al., 2019). Accumulating evidence over the last decade has convincingly shown that tau can be actively secreted from cells (Fá et al., 2016) and extracellular monomers, oligomers, or larger aggregates can be internalized by astrocytes and neurons *via* mechanisms that are not yet fully understood (Guo and Lee, 2014). The synaptotoxic action of ex-oTau relies on the ability of oligomers to enter neural cells. Once inside

the cell, oTau impinge on the molecular machinery serving for synaptic communication among neurons, including the release and uptake of glio/neuro-transmitters (Li Puma et al., 2022; Piacentini et al., 2017). Our previous studies documented that astrocytes upload ex-oTau more abundantly and rapidly than neurons, thus representing a primary target of ex-oTau. Once accumulated in astrocytes, oTau lead to alteration of intracellular Ca^{2+} signaling and intracellular Na^{+} overload that negatively affect Ca^{2+} and Na^{+}-dependent handling of neuro/gliotransmitters (e.g., ATP and glutamate), thus impinging on synaptic transmission (Li Puma et al., 2022; Piacentini et al., 2017). These findings support the view that astrocytes play a pivotal role in the disruption of synaptic function in tauopathies.

We also observed that the different internalization of oTau in astrocytes and neurons likely correlated with the different expression of heparan sulfate proteoglycans (HSPGs) (Li Puma et al., 2022). HSPGs are membrane receptors playing a critical role in protein trafficking through cell membrane (Holmes et al., 2013; Nazere et al., 2022; Song et al., 2022), and several studies have reported that internalization of oligomer species, including amyloid β (Aβ), α synuclein and tau proteins in neural cells is mediated by HSPGs and their modifications (e.g., 3-O or 6-O sulfation) (Mah et al., 2021; Rauch et al., 2018; Snow et al., 2021). HSPGs consist of long linear HS glycosaminoglycan (GAG) chains covalently attached to a core domain. They form a large family of extracellular receptors subdivided into three groups depending on their cellular localization: i) membrane HSPGs, such as syndecans and glycosylphosphatidylinositol-anchored proteoglycans (glypicans); ii) the secreted extracellular matrix HSPGs (agrin, perlecan, type XVIII collagen); and iii) the secretory vesicle proteoglycan, serglycin (Sarrazin et al., 2011). HSPGs are expressed in almost all cells, but they have a very important role in the development of central nervous system. Indeed, they are involved in the formation of specific synaptic connectivity patterns important for neural circuit function, and malfunction or altered expression of HSPGs may be involved in the pathophysiology of several brain disorders (Condomitti and de Wit, 2018), especially of neurodegenerative diseases caused by intracellular accumulation of misfolded proteins. Therefore, here we asked whether HSPGs and the control of its expression may play a critical role in the synaptotoxic action exerted by tau accumulation in astrocytes.

To date, which HSPGs are involved in tau oligomer internalization in astrocytes has not been identified yet. Our attention was focused on glypicans and, in particular, glypican 4 (GPC4), a glycosylphosphatidylinositol-anchored receptor expressed on the outer side of plasma membrane of several cells, including neurons and astrocytes in various brain areas. Indeed, astrocyte-secreted GPC4 has been reported to regulate tau hyperphosphorylation (Saroja et al., 2022), to mediate internalization of Aβ (Ma et al., 2021), as well as to promote formation of excitatory synapses (Allen et al., 2012; de Wit et al., 2013; Farhy-Tselnicker et al., 2017), that are the key target of extracellular tau oligomers. Here we report that GPC4 mediates ex-oTau internalization in astrocytes thus playing a critical role in the detrimental effects of ex-oTau on hippocampal glutamatergic synapses. We also found that the C-terminal domain of the amyloid precursor protein (APP) controls the expression of GPC4, thus highlighting the functional interplay between GPC4 and APP, that is also required for the entry, and for the consequent synaptotoxic action of ex-oTau (Piacentini et al., 2017; Puzzo et al., 2017).

Material and Methods

Primary cultures of hippocampal and cortical neurons and astrocytes

Primary cultures and co-cultures of hippocampal and cortical neurons and astrocytes were prepared from wild-type (WT) E18 C57BL/6 or APP TA (bearing a $Thr^{668}Ala$ mutation) mice, as previously described (Li Puma et al., 2021; Piacentini et al., 2017).

In brief, after brain removal, cortices and hippocampi were gently dissected in Phosphate Buffered Saline (PBS) at 4°C and then incubated for 10 min at 37°C in PBS containing trypsin–ethylenediaminetetraacetic acid 0.025%/0.01% w/v (Trypsin-EDTA, Biochrom AG, Berlin, Germany). Trypsin was inactivated with 1% fetal bovine serum (FBS) and the tissues were centrifugated and suspended in a dissociation medium consisting of 97.8% minimum essential medium (MEM, Biochrom), 1% FBS, 2 mM glutamine, 25 mM glucose and 1% penicillin–streptomycin-neomycin antibiotic mixture (PSN, Thermo Fisher Scientific, Waltham, MA). Tissues were then mechanically dissociated with a fire-polished Pasteur pipette at room temperature (RT) and then centrifuged at 235 × g for 10 minutes at RT. Cells were resuspended in the previously described medium added with 5% horse serum and 5% FBS and plated on poly-L-lysine (0.1 mg/mL, Sigma, St. Louis, MO)-pre-coated 20-mm coverslips (10^5 cells/well) for immunocytochemistry and FM1–43 imaging. After 24 hours from seeding (1 day *in vitro*, DIV), the culture medium was replaced with a fresh medium consisting of 96.5% Neurobasal medium (Thermo), 2% B-27 (Thermo), 2 mM glutamine and 1% PSN. After another 72 h (4 DIV), this medium was replaced with a glutamine-free version of the same medium, and the cells were grown for 10 more days before carrying-out experiments.

For primary cultures of hippocampal and cortical astrocytes, cells were resuspended in MEM with 3.7 g/L $NaHCO_3$ and 1.0 g/L D-glucose, 10% FBS, 1% PSN and then plated in flasks for cell expansion, on 20-mm coverslips (10^5 cells/well) for Ca^{2+} imaging and on 35-mm six-well plates (10^6 cells/well) for HPLC and Western blot (WB) analysis. The culture medium was changed after 24 h from seeding and twice weekly thereafter.

Organotypic hippocampal brain slices preparation

Hippocampal organotypic slice cultures were prepared from postnatal day 10 C57BL/6 mice using a McIllwain tissue chopper as previously described in (Piacentini et al., 2017; Renna et al., 2022). For each preparation 4 mice were used. At least 3 independent preparations were carried out. Slices (300 μm) were placed on semi-porous membranes (Merck Millipore, No. PCIMORG50, Burlington, MA) fed by tissue medium made of: 788 mL 1× MEM (Thermo), 7.16 g HEPES, 0.49 g $NaHCO_3$, 4.8 g D-glucose, 50 μl ascorbic acid (2.5%), 50 μL insulin (10 mg/ml), 200 mL horse serum (Thermo), 2 mL $MgSO_4$ (1 M), 1 mL $CaCl_2$ (1 M). Slices were incubated at 35°C in 5% CO_2 and cultured for up to 4 days before treatment for 24 hours with vehicle or anti-GPC4 antibody and 1-hour incubation with 200 nM ex-oTau.

Assessment of tau uploading into cultured neurons and astrocytes

Recombinant human tau was prepared as previously described in (Piacentini et al., 2017) and (Li Puma et al., 2022). Fluorescent oligomeric tau was prepared by labeling with the active ester dye IRIS-5-NHS (IRIS 5; λ_{ex}: 633 nm; λ_{em}: 650–700 nm; Cyanine Technology, Turin, Italy), as previously described (Fá et al., 2016). In brief, 2 mM tau solution in PBS were combined with 6 mM IRIS-5 in dimethyl sulfoxide (DMSO) and incubated for 4 h in the dark under mild shaking conditions. Then, Vivacon 500 ultrafiltration spin columns (Sartorius Stedim Biotech GmbH, Goettingen, Germany) were used to purify labelled tau. Purified tau was resuspended in PBS and used at a final concentration of 200 nM. Immunocytochemistry and confocal microscopy were performed in astrocytes treated with ex-oTau^{IRIS-5} 200 nM for 1 h or 6 h, after a 24h-pre-treatment with anti-GPC4 antibody at dilution of 1:300 or 1:600 (see “Glypican 4 antibody treatment” paragraph), or vehicle. All experiments were repeated at least three times. To quantify the amount of cellular internalization of tau the parameter “internalization index” was introduced by multiplying the percentage of astrocytes internalizing fluorescent proteins in each analyzed microscopic field by the mean number of fluorescent spots inside cells. For a subset of experiments, we also evaluated internalization of Aβ42 in cultured astrocytes treated with anti-GPC4. Aβ42 tagged with HyLite fluor 555 (Aβ42^{555}) was prepared and used as already described in Puzzo et al., 2017.

Glypican 4 antibody treatment

In order to evaluate the dependence of oTau entry on the expression of GPC4, we treated cell cultures (pure culture of astrocytes, co-cultures neurons and astrocytes, and organotypic brain slices containing hippocampus) with an anti-GPC4 antibody (Bioss Inc.; recognizing the immunogen sequence DVKEKLKQAKKF which are amino acids 388–399 of GPC4, out of 556 total). The stock concentration of the antibody was 1 μg/μL and it was used at the final concentration of 3.4 ng/μL (1:300 dilution). A subset of experiments, aimed at evaluating the efficacy of lower concentration of antibody in preventing oligomeric tau entry were conducted by treating cells for 24 hours with the antibody at 1:600 dilution (1.7 ng/μL).

Confocal Ca^{2+} imaging

To perform Ca^{2+} imaging, astrocytes were incubated for 30 min at 37°C with 2.5 μM Fluo-4-AM (Thermo), a Ca^{2+} sensitive fluorescent dye, in Tyrode’s solution. This solution consisted of NaCl (150 mM), glucose (10 mM), HEPES (10 mM), KCl (4 mM), $CaCl_2$ (2 mM) and $MgCl_2$ (1 mM) and its pH was adjusted to 7.4 with NaOH. Cells were then maintained in fresh Tyrode’s solution at RT for 20 min to allow dye de-esterification.

Intracellular Ca^{2+} transients were elicited by exposing Fluo-4-AM-loaded cells to ATP (100 μM) for 10 s. Fluo-4-AM was excited at 488 nm and its emission signal was collected between 500 and 550 nm with an inverted laser scanning confocal system Leica TCS-SP5 (Wetzlar, Germany).

The amplitude of each Ca^{2+} signal was estimated in a semi-quantitative way by the following formula: $\Delta F/F = (F_t - F_{pre})/(F_{pre} - F_{bgnd})$, where F_t is the mean of fluorescence

intensities measured in a region of interest (ROI) drawn around each cell body at a given time (t); F_{pre} is the basal fluorescence intensity in this ROI estimated as mean value of fluorescence during 20-s prior ATP exposure; F_{bgnd} is background fluorescence intensity measured in an area lacking dye-filled cells.

High-performance liquid chromatography (HPLC)

For HPLC measurements WT astrocytes were cultured in 35-mm six-well plates and pre-treated for 24h with anti-GPC4 antibody or vehicle in their culture medium. After antibody treatment (at dilution 1:300 or 1:600), cells were treated for 1 hour with vehicle, or ex-oTau 200 nM in Tyrode's solution at 37 °C. At the end of treatment, cells and supernatants were separately collected and treated for HPLC measurements as already done in (Piacentini et al., 2017) and (Li Puma et al., 2022). Tyrode's solution was withdrawn from each well and deproteinized according to (Tavazzi et al., 2005). Briefly, supernatant samples were transferred to an Eppendorf tube equipped with a filtering membrane of 3KDa cut-off (Nanosep® Centrifugal Devices, Pall Gelman Laboratory, Ann Arbor, MI, USA) and centrifuged at 10,500 × g for 15 min at 4 °C. The protein-free ultrafiltrate samples were directly injected into the HPLC column and analyzed to determine extracellular ATP concentrations released by astrocytes in the culture media, according to an ion-pairing HPLC method previously set up (Piacentini et al., 2017; Tavazzi et al., 2005). Separation and quantification of ATP was carried out using a Hypersil 250 × 4.6 mm, 5 μm particle-size column, which was provided with its own guard column (Thermo). The HPLC apparatus consisted of a Surveyor System that was connected to a highly sensitive PDA diode-array detector (Thermo), equipped with a 5-cm light-path flow cell and set up to acquire signals between 200 and 300 nm wavelengths. The data were acquired and analyzed by a PC using the ChromQuest® software package that was provided by the HPLC manufacturer. The concentrations of ATP in culture media were determined at 260 nm wavelength by matching retention times, peak areas and absorption spectrum of those of freshly prepared ultrapure standard solutions.

FM1–43 imaging

FM1–43 imaging was performed as previously described (Piacentini et al., 2017). Briefly, co-cultures of hippocampal neurons and astrocytes plated on 20-mm coverslips were treated with vehicle or anti-GPC4 antibody for 24 hours before be treated with vehicle or ex-oTau for 1 hour. After treatment, cells were placed in Tyrode's solution for 1 min and then exposed for 30 s to 5 μM FM1–43 (Thermo) in Tyrode's solution. After this time, cells were placed for 1 min in 5 μM FM1–43 in depolarizing 50 mM KCl Tyrode's solution, which induced massive vesicle release and vesicle staining with FM1–43. After that, cells were placed again in standard Tyrode's solution containing 5 μM FM1–43 for 30 s and then in Tyrode's solution containing 200 mM Advasep™-7 (Sigma) for 2 min. FM1–43 fluorescence was excited by Argon laser at 488 nm and fluorescence was recorded in a spectral window ranging from 520 to 650 nm with a Leica TCS-SP5 confocal system (Leica). FM1–43 de-staining was obtained by re-exposing FM1–43 labelled cells to 50 mM KCl for 1 min in Tyrode's solution.

Immunocytochemistry

Astrocytes for immunocytochemistry were treated as follow: i) with vehicle or with anti-GPC4 antibody (at 1:300 and 1:600 dilutions) for 24 h and then with 200 nM fluorescent-tagged ex-oTau^{IRIS-5} for 1 h or 6 h, at 37°C; ii) with vehicle or with 2 μM γ-secretase inhibitor X (565771, Sigma) for 48 h; iii) with vehicle or with 200 nM ex-oTau for 1 h, after a 24h-pretreatment with anti-GPC4 antibody or not.

Cells were fixed with 10% formalin solution (pH 7.4 with NaOH) for 10 min at RT and then permeabilized with 0.3% Triton X-100 (Sigma) in PBS for 15 min. To block non-specific binding sites, cells were incubated in 0.3% BSA in PBS for 20 minutes at RT. Cells were incubated overnight at 4 °C with an appropriate combination of the following antibodies, diluted in the same blocking solution: mouse anti-GFAP (#3670, 1:500, Cell Signaling Technology, Danvers, MA) or rabbit anti-GFAP (#12389, 1:500, Cell Signaling), and mouse anti-Heparan Sulfate (10E4 epitope, USbiological) or rabbit anti-GPC4 (bs-2159R, 1:300, Bioss, Boston, MA); mouse anti-MAP2 antibody (1:300, Sigma); rabbit anti-Synapsin-1 (#5297, 1:300, Cell Signaling). After primary antibodies removal, cells were washed in PBS and then incubated for 90 min at RT with the proper secondary antibodies, diluted in the blocking solution: Alexa Fluor 546 donkey anti-mouse and Alexa Fluor 488 donkey anti-rabbit (both used 1:1000, Thermo). Finally, cells were incubated with 4',6-diamidino-2-phenylindole (DAPI, Thermo), 0.5 mg/mL in PBS for 10 minutes at RT, in order to counterstain their nuclei. Cells were then coverslipped with ProLong Gold anti-fade reagent (Thermo) and studied by confocal microscopy.

Confocal stacks of images (1024×1024 pixels) were acquired at 60× magnification with a confocal laser scanning system Nikon A1MP (physical pixel size: 210 nm).

Hippocampal slices preparation and immunohistochemistry

Hippocampal slices were obtained from 5-month-old C57BL/6 mice, as previously described (Li Puma et al., 2019), with minor modifications. Mice were deeply anesthetized with a cocktail of ketamine (100 mg/mL) and medetomidine (1 mg/mL) in a 5:3 ratio, and perfused transcardially with PBS followed by 4% (w/v) PFA fixative solution. Brains were removed from the skull and post-fixed overnight at 4 °C; then, they were transferred into a 30% sucrose solution in PBS for 2 days. Tissue was sectioned coronally (40 μm) with a vibratome (VT1000S; Leica), and stored in cryoprotectant at −20 °C.

After three rinses in PBS, the sections were incubated for 1 hour at RT in a blocking solution consisting of 1% bovine serum albumin, 10% normal goat serum, and 0.5% Triton X-100. Immunohistochemistry was performed on a one-in-six series of equidistant (240 μm between sections) free-floating sections by using the following antibodies: mouse anti-GFAP antibody (#3670, 1:300, Cell Signaling) and rabbit anti-GPC4 antibody (bs-2159R, 1:300, Bioss). The fluorescent secondary antibodies Alexa Fluor 546 donkey anti-mouse (1:500) and Alexa Fluor 488 donkey anti-rabbit (1:500) were then used. Cell nuclei were counterstained with DAPI (0.5 μg/mL) and the sections were mounted on glass slides and coverslipped with ProLong Gold antifade reagent. Confocal stacks of images were acquired

at 40× magnification with a confocal laser scanning system Nikon A1MP (physical pixel size: 210 nm).

Western blot

Protein extraction was performed with RIPA buffer, added with 1 mM phenylmethylsulfonyl fluoride (PMSF), sodium fluoride (NaF), sodium orthovanadate (Na_3VO_4), and protease inhibitor mixture. Homogenates of both cells and tissues were sonicated and centrifuged at 13,000 × g for 15 min at 4°C. The supernatants were collected, and their protein concentration was assessed by Bradford protein assay. Equivalent protein samples were loaded onto 8% tris-glycine polyacrylamide gel for electrophoresis separation (Running buffer: 10% Tris/Glycine and 0.1% SDS). Proteins were then electroblotted onto nitrocellulose membranes for Western blot analysis (Transfer buffer: 10% Tris/Glycine and 20% methanol). Membranes were blocked with 5% non-fat dry milk in tris-buffered saline containing 0.1% Tween-20 for 1 hour at RT and then incubated overnight at 4°C with the following primary antibodies (all diluted 1:500): rabbit anti-GPC4 (bs-2159R, Bioss), rabbit anti-Synapsin-1 (#5297, Cell Signaling Technology), mouse anti-Synaptophysin (ab8049, Abcam), rabbit anti-GluA1 (Ab-849, SAB, Baltimore, MD, USA). Housekeeping proteins, mouse anti-tubulin (Sigma) and mouse anti-GAPDH (Abcam) were used at 1:1,000. The next day, membranes were incubated with appropriate secondary horseradish peroxidase-conjugated antibodies (1:2,500, Cell Signaling) for 1 hour at RT. Visualization was performed with WESTAR ECL (Cyanagen, Bologna, Italy), using UVItec Cambridge Alliance. Molecular weights for immunoblot analysis were determined through Precision Plus Protein™ Standards (BioRad, Hercules, CA). Densitometric analysis was carried out with UVItec software. Experiments were repeated at least three times.

Original uncropped gel and/or Western blot analysis are available in the Supplementary Information.

Electrophysiology in organotypic hippocampal slices

Hippocampal subfields and electrode positions were identified with 4× and 40× water-immersion objectives on an upright microscope equipped with differential interference contrast optics under infrared illumination (BX51WI; Olympus) and video observation (BTE-B050-U CMOS camera; Mightex). Schaffer collateral fibers were stimulated with a bipolar tungsten electrode (FHC, Bowdoin, ME, USA). Slices were incubated in ACSF gassed with 95% O_2/5% CO_2. All experiments were performed at RT. Patch pipettes had a resistance of 4–6 MΩ when filled with an internal solution containing (in mM): 135 $CsMeSO_3$, 8 NaCl, 10 HEPES, 0.25 EGTA, 2 Mg_2ATP, 0.3 Na_3GTP, 0.1 spermine, 7 phosphocreatine, and 5 QX-314, pH 7.25–7.30, 294–298 mOsm. After establishing a gigaseal, the patch was broken by applying negative pressure to achieve a whole-cell configuration. A series resistance lower than 15 MΩ was considered acceptable and constantly monitored throughout the entire recording. Excitatory Post Synaptic Currents (EPSCs) were recorded in voltage-clamp configuration, with CA1 pyramidal neurons held at −70 mV. The stimulation intensity that elicited 1/3 of the maximal response was used for delivering test pulses every 10 seconds. Long-Term Potentiation (LTP) was induced by two trains of High Frequency Stimulation (HFS; 100 Hz, 1 s) separated by 20 s, while cells

were depolarized to 0 mV. This induction protocol was always applied within 5–7 min from achieving the whole-cell configuration, to avoid "*wash-out*" of LTP. Responses to test pulse were recorded for 30 min to assess LTP. The amplitudes of EPSCs at 30 min were averaged from values obtained during the last 5 min of post-HSF recordings (from min 25 to min 30). LTP magnitude was expressed as the percentage change in the mean EPSC peak amplitude normalized to baseline values = 100% (i.e., mean values for the 5 minutes of recording before HFS). The electrophysiological recordings were analyzed using the Clampfit 10.9 software (Molecular Devices).

Chromatin Immunoprecipitation and qPCR

Chromatin immunoprecipitation (ChIP) assay was performed as previously described (Leone et al., 2019), with minor modifications. Hippocampal and cortical tissues were homogenized in 200 μL of lysis buffer, made of 1% SDS, 50 mM Tris-HCl pH 8.0, and 10 mM EDTA, and sonicated on ice with 10 s pulses at 10 s interpulse interval for 20 minutes. Sample debris was removed by centrifugation and supernatants were precleared with protein G-agarose beads (Sigma-Aldrich) for 1 h at 4 °C. Two micrograms of specific antibody or control IgG were added overnight at 4 °C. Immune complexes were collected by incubation with protein G-agarose beads for 4 h at 4 °C. Immunoprecipitated complexes were repeatedly washed and then separated from beads in 150 μL of elution buffer (1% SDS and NaHCO3 0.1 M; pH 8.0). After the addition of NaCl, lysates were incubated overnight at 65 °C to reverse protein-DNA cross-linking. Chromatin fragments were extracted with PCR DNA fragments purification kit (Geneaid Biotech Ltd., New Taipei City, Taiwan).

Real time qPCR conditions and cycle numbers were determined empirically. Data are expressed as a percentage of input calculated by the "adjusted input value" method according to the manufacturer's instructions (Thermo Fisher Scientific ChIP analysis). To calculate the adjusted input, the Ct value of input was subtracted by 6.644 (i.e., log2 of 100). Next, the percent input of control and IP samples was calculated using the formula: 100 × 2^(adjusted input − Ct(ChIP)). The percent input of IgG samples was calculated using the formula 100 × 2^(adjusted input − Ct(IgG)).

The primers used for GPC4 promoter analysis are indicated below:

1st region (bp −150/−1): Fw 5'-CCTCATGCCCGCCCCCTC-3'; Rv 5'-CTGCTCCGCTCACCCAGCCC-3';

2nd region (bp −275/−125): Fw 5'-GTCGCAAGAGGGAGCGCCG-3'; Rv 5'-CCCTAAGGGAGGGAGGGGG-3'.

Statistics

Statistical comparisons and analyses were carried out with SigmaPlot software 14.0. Data samples were subjected to normal distribution assay and then expressed as mean ± standard error of the mean (SEM). Two-tailed Student's t test and one-way ANOVA with Bonferroni's or Dunnet's *post-hoc* tests were used for comparing two or many experimental groups, respectively. The Mann–Whitney (Wilcoxon) nonparametric statistic was used when

experimental data were fewer than 10 observations. The level of significance (p) was set at 0.05.

Ethics approval

All animal procedures were approved by the Ethics Committee of Università Cattolica (#63/2019-PR) and were fully compliant with Italian (Ministry of Health guidelines, Legislative Decree No. 116/1992) and European Union (Directive No. 86/609/EEC) legislations on animal research.

Results

Anti-GPC4 antibody prevents ex-oTau internalization in astrocytes

We previously demonstrated that after 1-hour treatment of co-culture of murine hippocampal neurons and astrocytes with 200 nM ex-oTau tagged with a fluorophore (IRIS-5, Cyanine Technologies) numerous fluorescent spots indicating oTau were found inside astrocytes whereas none or very few were in neurons (Piacentini et al., 2017). In the present study we took advantage of this experimental paradigm to dissect the effects of tau accumulation in astrocytes from the overall detrimental action of tau in the brain, and to assess the role of GPC4 in the astrocytic internalization of oTau, and their following synaptotoxic action. We first investigated the expression of GPC4 in cultured hippocampal astrocytes and in astrocytes of mouse hippocampal slices from WT C57BL/6 mice by immunofluorescence (IF) and WB experiments (Supplementary Figure S1A,B and S3D,E). After, we tested the effects of counteracting the interaction between oTau and GPC4 on ex-oTau internalization. We found that 24-h treatment of cultured hippocampal astrocytes with the anti-GPC4 antibody (binding the receptor on its extracellular side) at concentration of 3.4 ng/μL (1:300 dilution) before 1-h application ex-oTau (200 nM) significantly reduced the cellular uploading of ex-oTau tagged with IRIS-5 (Figure 1A,B). Internalization index (as defined in (Piacentini et al., 2017)) revealed a 43% reduction of oTau uploading in anti-GPC4-treated cells (from 1.00±0.09 to 0.57±0.03 for untreated vs. antiGPC4-treated cells, respectively; $p=1.7\times10^{-4}$, assessed by Student's t test). We also generated "internalization maps", i.e., a two-dimensional picture showing co-localization between IRIS-5-tagged oTau and astrocyte-specific glial fibrillary acidic protein (GFAP), indicating oTau internalization as black dots (Figure 1A2-B2) further demonstrating the effect of anti-GPC4 antibody in impeding oTau uploading. In order to validate the efficacy of anti-GPC4 antibody against oTau internalization we treated astrocytes with oligomeric tau for times longer than 1 hour. In particular, we choose 6 hours that is the minimum time period allowing a detectable tau entry also in neurons (Fà et al., 2015). As expected, the amount of oTau entering astrocytes after this longer exposure was higher than that observed after 1 hour (+113%; $p=5.4\times10^{-4}$) but antibody treatment still reduced tau internalization by 37% (p=0.02; Supplementary Figure S2A-C,F). We also evaluated the efficacy of a lower concentration of antibody in preventing tau entry. Specifically, we used 1.7 ng/μL (1:600 dilution) that corresponds to the concentration commonly used to reveal the receptor by WB analysis. Under these experimental conditions the amount of oTau uploaded by astrocytes was highly variable, and the effects of treatment were not statistically significance (Supplementary Figure S2C,D,F). To test whether oTau entrance was affected by temperature, a subset of experiments was

repeated by applying oTau in cells maintained at +4 °C. In these conditions oTau did not enter astrocytes (Supplementary Figure S2E,F).

Finally, we wondered if the ability of anti-GPC4 in preventing oligomers internalization was specific for oTau or it also inhibited uploading of other oligomeric species. Based on previous literature reports (Ma et al., 2021), we evaluated the efficacy of anti-GPC4 (1:300) in preventing uploading of 200 nM Aβ42 applied for 1 hour to cultured astrocytes, and found that the antibody also strongly inhibited Aβ42 internalization (Supplementary Figure S3).

Treatment with anti-GPC4 antibody prevents ex-oTau-induced alteration of intracellular calcium signaling in astrocytes and restores gliotransmitter release from oTau-targeted astrocytes

One-hour treatment of cultured hippocampal astrocytes with ex-oTau markedly reduced intracellular Ca^{2+} transients induced by application of ATP, as well as the frequency and amplitude of spontaneous intracellular Ca^{2+} waves observed after ATP stimulation (Piacentini et al., 2017). We also reported that these effects depended on oTau accumulation in astrocytes. Here we found that cell treatment with anti-GPC4 (3.4 ng/μL; 1:300), besides reducing ex-oTau uploading in astrocytes, also prevented ex-oTau-mediated impairment of Ca^{2+} transients elicited by ATP exposure. In fact, compared to control conditions (i.e., vehicle-treated astrocytes), the peak amplitude of intracellular Ca^{2+} transients induced by 10-s ATP (100 μM) stimulation in 1-h-ex-oTau-treated astrocytes was reduced by 58±1% (ANOVA test with Bonferroni *post-hoc* correction: $F_{2,1333} = 275.72$; $p<0.001$ vs. vehicle), in agreement with our previous reports (Piacentini et al., 2017). However, when ex-oTau application was preceded by 24-h cell pre-treatment with anti-GPC4 the ex-oTau-induced reduction in amplitude of intracellular Ca^{2+} transients was only 13±1%, and not significantly different from vehicle (Figure 2A). Similarly, the mean number of spontaneous Ca^{2+} transients/min observed after ATP application, that was significantly reduced by ex-oTau application (−43%; $p<0.01$), returned to values similar to controls following cell preincubation with anti-GPC4 antibody (Figure 2B). In agreement with data obtained in immunofluorescence experiments, cell pretreatment with a lower concentration (1.7 ng/μL; 1:600) of the antibody produced a lower, but still statistically significant, effect in preventing the reduction of intracellular Ca^{2+} transient amplitude (Supplementary Figure S4A).

Intracellular Ca^{2+} signals in astrocytes regulate the release and uptake of glio/neurotransmitters acting as neuromodulators for synaptic communication among neurons (Lalo et al., 2016; Perea and Araque, 2010). In our previous study (Piacentini et al., 2017) we reported that ex-oTau treatment impaired the release of gliotransmitters such as ATP and glutamate, with the former being the most affected one (c.a. 70% reduction vs. controls). Therefore, we wondered if anti-GPC4 treatment also reverted the detrimental effects of ex-oTau application on spontaneous release of ATP from astrocytes. In agreement with our previous data, HPLC experiments revealed that the amount of extracellular ATP measured in the culture media of oTau (1-h)-treated astrocytes was significantly lower than in vehicle-treated ones (−58%; from 0.074±0.18 μM to 0.033±0.007 μM, $p=0.032$; assessed by Student's t test; Supplementary Figure S4B) but if oTau treatment was preceded by

culture incubation with anti-GPC4 (1:300), the amount of extracellular ATP released by astrocytes in the culture medium was not significantly different from controls (0.075±0.026 μM; p=0.97 vs. vehicle; Figure 2C). As already observed for Ca^{2+} transients, when antibody was used at a lower concentration (1:600), its effect in preventing impairment of ATP release was smaller although statistically significant (0.055±0.002 μM; p=0.97 vs. vehicle; Supplementary Figure S4B). Anti-GPC4 alone (1:300) did not significantly affect the spontaneous release of ATP (0.069±0.024 μM; p=0.86 vs. vehicle). The effect of ex-oTau on astrocytes pre-treated with anti-GPC4 were similar to those observed in astrocytes derived from APP KO mice that we already demonstrated to be unable to upload ex-oTau (Li Puma et al., 2022; Piacentini et al., 2017). Indeed, the amount of extracellular ATP released in the medium of these cells after 1-h ex-oTau treatment was significantly larger than that observed in cells in which oTau can enter and accumulate (0.056±0.007 vs. 0.031±0.008 μM; p=0.034 assessed with Mann-Whitney test), and not significantly different from vehicle-treated cells (p=0.87; Supplementary Figure S4C).

Anti-GPC4 antibody spares synapses from the detrimental action of ex-oTau

We previously demonstrated that reduced Ca^{2+}-dependent release of gliotransmitters, and ATP in particular, from oTau-targeted astrocytes mediates the synaptotoxic action of 1-h application of ex-oTau in neurons co-cultured with astrocytes. Indeed, restoration of extracellular ATP spared neurons from the deleterious effects of ex-oTau (Piacentini et al., 2017). We then asked if the treatment with anti GPC4 antibody was also effective in protecting neurons, and in particular synapses, from the detrimental astrocyte-mediated action of oTau. By taking advantage of the experimental paradigm of 1-h lasting ex-oTau application (200 nM), allowing tau accumulation in astrocytes only, we treated co-cultures of hippocampal neurons and astrocytes that were previously incubated for 24 hours with either anti-GPC4 or vehicle and evaluated the efficiency of synaptic vesicle release by FM1–43 imaging. In agreement with previously published data (Piacentini et al., 2017), we found that 1-h lasting ex-oTau treatment significantly reduced the amount of synaptic vesicles released after a depolarizing stimulus (consisting of 10-s exposure to 50 mM KCl in Tyrode's solution) (Figure 3A), even if it did not affect the release rate. This conclusion was obtained by fitting the FM1–43 fluorescence intensity curves with an exponential function ($y=A\times e^{-(t/\tau)}$; Figure 3B), where A represents the initial amount of synaptic vesicles, "t" is the time, and the time constant "τ" represents the release rate. Significant differences between vehicle and oTau treatment were observed only for the factor A (one-way ANOVA test: $F_{2,106}=14.11$, $p<0.001$; n=28 neurons analyzed for vehicle/vehicle; n=18 for vehicle/ex-oTau), but not for the time constant τ (one-way ANOVA test: $F_{2,106}=1.87$, p=0.16). Twenty-four-hour pre-treatment of co-cultures of hippocampal neurons and astrocytes with anti-GPC4 prevented the effects of oTau on synaptic vesicle release (Figure 3A,B), without exerting any significant effect on vehicle-treated cells.

Pre-treatment of cultures with the anti-GPC4 antibody also reverted the detrimental effects of ex-oTau on expression of synaptic proteins. In hippocampal neurons co-cultured with astrocytes 1-h treatment with ex-oTau (200 nM) significantly reduced synapsin-1 immunoreactivity by 41% vs. vehicle, but 24-h antibody treatment prior to ex-oTau application produced a rescue of about 63% vs. ex-oTau (Figure 3C,D; $p=7.2\times10^{-7}$ assessed

by one way ANOVA followed by Bonferroni *post-hoc* test). Of note, these effects were not confined to an *in vitro* model, but they were confirmed in organotypic hippocampal slices. In this experimental model we first documented a significant reduction of the expression of pre- and post-synaptic proteins induced by 1-h ex-oTau (200 nM) treatment by WB experiments (specifically, −44% for synapsin-1; −47% for synaptophysin and for the GluA1 subunit of AMPA receptor; $p<0.05$ assessed by Student's t test). On the contrary, no significant decrease in expression of these proteins was found when slices were pre-treated for 24 h with anti-GPC4 antibody before exposure to ex-oTau (Figure 3E,F).

LTP recordings further confirmed the protective effect of anti-GPC4 against the synaptic damages induced by ex-oTau at CA3-CA1 synapses in organotypic hippocampal slices. In agreement with our previous data obtained in acutely isolated hippocampal slices (Fá et al., 2016; Puzzo et al., 2017), 1 hour exposure to ex-oTau (200 nM) significantly reduced LTP amplitude at the CA3-CA1 synapse (−48%; $p=0.03$ assessed by one-way ANOVA followed by Dunnet's *post-hoc* test). However, no significant differences were found between LTP amplitudes recorded in organotypic hippocampal slices exposed to either vehicle or ex-oTau (200 nM) following 24 h-treatment with anti-GPC4 antibody (Figure 4A,B). Notably, brain slice treatments with the antibody alone did not exert any significant effect on LTP ($p=0.9$ vehicle vs. anti-GPC4).

HSPGs and GPC4 expression depends on Amyloid Precursor Protein

Having previously demonstrated that the expression of APP is required for the entry and the consequent synaptotoxic action of ex-oTau (Piacentini et al., 2017; Puzzo et al., 2017), we investigated the relationship between APP and HSPGs. To this aim we evaluated the expression of HSPGs and GPC4 in hippocampal brain slices and cultured astrocytes of WT and APP KO mice through IF and WB experiments. We found that APP KO hippocampal tissue expresses lower levels of HSPGs and, in particular, of GPC4 with respect to APP WT ones. Specifically, IF analysis performed on cultured astrocytes from APP KO mice revealed a reduction of HSPG immunoreactivity of −84% vs. cells from APP WT ones (from 100±8.3 to 16±3.7; $p=2.1\times10^{-6}$, assessed with Student's t test; Supplementary Figure S5A-C). With specific reference to GPC4, we assessed its expression in both cultured astrocytes and brain tissues of APP WT vs. APP KO mice. Confocal microscopy analyses revealed a marked reduction of GPC4 immunoreactivity in hippocampal sections from APP KO mice, especially in GFAP-reactive astrocytes, respect to WT ones (Figure 5A,B). WB analyses carried out on lysates from both cultured astrocytes and whole hippocampal tissues of APP WT vs. APP KO mice also revealed a reduction of GPC4 expression in terms of both protein [−46±9% with respect to APP WT in cultured cells ($p=0.029$ assessed by Rank Sum test; Supplementary Figure S5D,E), and −48±9% in whole hippocampal tissues ($p=0.031$ assessed by paired Student's t test; Figure 5C,D] and mRNA (−38±5%; Figure 5E; $p=0.0101$). Notably, APP KO mice exhibiting low GPC4 levels were also quite insensitive to the synaptotoxic action of ex-oTau (Piacentini et al., 2017; Puzzo et al., 2017), thus supporting our hypothesis that GPC4 is one of the main determinants of ex-oTau synaptotoxicity.

Based on data shown above, we asked how the presence of APP might modulate the expression GPC4. It is known that the C-terminal domain of APP (Amyloid Intracellular Domain – AID (Passer et al., 2000), also called AICD), produced by the γ-secretase-mediated proteolytic processing of APP, acts as a transcription factor for several genes once translocated to the nucleus (Bukhari et al., 2017; Chang et al., 2006; Müller et al., 2008). To check whether GPC4 expression depended on AICD, we first studied the expression levels of HSPGs and GPC4 in cultured APP WT astrocytes that were treated for 48 hours with γ-secretase inhibitors: either the InSolution™ γ-secretase inhibitor X (2 μM, Calbiochem) or the ELND006 (5 μM, Sigma-Aldrich). Results from IF and WB experiments showed that the treatment of cultured WT astrocytes with the γ-secretase inhibitors X significantly reduced immunoreactivity of HSPGs (−29%, $p=5\times10^{-4}$ assessed by Student's t test; Supplementary Figure S5F-H) and GPC4 (−30%, p=0.049; Figure 5F-H), compared to vehicle (i.e., DMSO)-treated cells. Similar results were obtained by WB analysis in cultured astrocytes treated with ELND006 (−31±17%, p=0.029 assessed by Mann-Whitney test; Figure 5I,J). A regulatory function of AICD on GPC4 expression was also supported by ChIP experiments showing that AICD binds the promoter of the *Gpc4* gene (Figure 5K).

AICD formation and its nuclear translocation depend on phosphorylation at Thr668 which is located at the intracellular C-terminus of APP. Thr668 phosphorylation triggers γ-secretase cleavage of APP and favours the formation of a complex involving AICD and other two regulatory proteins, Tip60 and Fe65, that are necessary for AICD translocation to the nucleus (von Rotz et al., 2004). To further check our hypothesis that GPC4 expression depends on phosphorylation-dependent APP processing, we assessed the expression levels of GPC4 in hippocampal tissue and cultured cortical astrocytes obtained from transgenic mice in which threonine 688 of APP was substituted by the non-phosphorylatable amino acid alanine (APP^{TA} mice, (Lombino et al., 2013)). Immunofluorescence experiments carried out in brain slices containing hippocampus suggested that the expression of GPC4 was significantly reduced in APP^{TA} mice (Figure 6A,B), and this result was confirmed by quantitative WB analysis performed on hippocampal lysates (−47±8%, p=0.013; Figure 6C,D) and in terms of mRNA in experiments carried out on cortical astrocytes (−43±6%: p=0.006; Figure 6E).

Taken together, our data indicate that in experimental models in which either AICD formation is prevented (APP KO or γ-secretase inhibition) or its phosphorylation at Thr668 is impeded (APP^{TA} mice), the expression of GPC4 is significantly reduced, thus suggesting a central role for this oligopeptide in *Gpc4* gene transcription, GPC4 expression, ex-oTau entry, and tau synaptotoxicity.

Discussion

Extracellular tau oligomers have been reported to affect synaptic transmission, synaptic plasticity, and memory in WT C57BL/6 mice (Fá et al., 2016; Lasagna-Reeves et al., 2011; Piacentini et al., 2017; Puzzo et al., 2017). We demonstrated that the synaptotoxic effects of ex-oTau strongly depend on their internalization in neural cells (Fá et al., 2016), with a significant contribution given by astrocytes (Li Puma et al., 2022; Piacentini et al., 2017). The latter observation was obtained by using a particular experimental

paradigm consisting of a short-lasting (i.e., 1-hour) treatment with ex-oTau allowing us to dissect the effects of ex-oTau mediated by their internalization in astrocytes from those depending on ex-oTau uploading in neurons. Indeed, after 1-hour treatment of murine hippocampal co-cultures of neurons and astrocytes or organotypic hippocampal slices with 200 nM ex-oTau only astrocytes showed significant intracellular accumulation of oTau, whereas neurons contained none or very low amounts of these oligomers (Piacentini et al., 2017). Several tau internalization pathways have been identified so far, mainly depending on the protein aggregation forms (monomers, oligomers, fibrils). They include macropinocytosis, Clathrin-mediated endocytosis, lipid raft-dependent endocytosis, tunneling nanotubes-dependent endocytosis, and phagocytosis (Zhao et al., 2021). However, the HSPG-dependent endocytosis seems to be the predominant mechanism of internalization of tau aggregates, and it depends on GAG length and sulfation patterns such as 3-O-sulfation and 6-O sulfation (Holmes et al., 2013; Kolay et al., 2022; Rauch et al., 2018; Song et al., 2022; Stopschinski et al., 2018; Zhao et al., 2021). In a previous study we documented that astrocytes express higher levels of HSPGs than neurons (Li Puma et al., 2021), thus possibly explaining their greater ability to upload extracellular tau oligomers. Here we demonstrated that among the various receptors belonging to the family of HSPGs, the glypican 4, whose expression in astrocytes is of fundamental importance for the functional development of glutamatergic synapses (Allen et al., 2012; Farhy-Tselnicker et al., 2017), is a key receptor for oTau entry in astrocytes and its consequent synaptotoxic action. Indeed, because ex-oTau entry in astrocytes produces a synaptotoxic action via altered neuro/gliotransmitter release and uptake (Li Puma et al., 2022; Piacentini et al., 2017), counteracting the interaction between ex-oTau and GPC4 by a specific antibody binding the receptors on their extracellular side, prevents ex-oTau internalization in astrocytes and the following detrimental effects they exert on synaptic function. Our finding is in agreement with very recent literature reports showing that tau uptake is mediated by the low-density lipoprotein receptor-related protein 1 (LRP1) (Rauch et al., 2020), and GPC4 interacts with APOE4 to regulate tau hyperphosphorylation (Saroja et al., 2022) and with LRP1 to allow the internalization of oligomeric species (Ma et al., 2021).

We found that 24-h treatment of hippocampal cell cultures (either astrocytes or co-cultured neurons and astrocytes) or hippocampal brain slices with anti GPC4 antibody at the concentration of 3.4 ng/mL was effective in preventing tau internalization in astrocytes, independently on the time of application of extracellular tau oligomers. In particular, after 1 hour of oTau treatment GPC4 antibody spares: i) alterations of intracellular Ca^{2+} signals and ATP release from astrocytes that, triggering further release of ATP by a mechanism defined “ATP-induced ATP release” (Xiong et al., 2018), fuels synaptic transmission by binding its specific receptors on the plasma membrane of pre- and post-synaptic neurons (Guzman and Gerevich, 2016; Koizumi et al., 2003); ii) the reduction of synaptic vesicular release and synaptic protein expression in neurons co-cultured with astrocytes; iii) inhibition of hippocampal LTP at CA3-CA1 synapses. Notably, the antibody alone had no significant effects on LTP. However, it is important to note that in these experiments brain slices were exposed to the antibody only during vehicle or ex-oTau treatment, but not during the EPSC recordings, including the potentiation protocol (pairing stimuli). This is important in the light of data reported by (Allen et al., 2012) showing that astrocyte-released GPC4

is important for the clustering of AMPA receptors and the functional development of glutamatergic synapses.

Our experimental paradigm, greatly favoring tau accumulation in glial cells rather than in neurons, clearly indicates that ex-oTau entry in astrocytes via GPC4 is a major determinant of the synaptotoxic action exerted by this molecular hallmark of AD. Of course, on a longer time scale, ex-oTau also enter and accumulate in neurons where they exert their detrimental effects by acting on different targets. We previously reported that, after several hours of incubation with ex-oTau, neurons accumulate significant amounts of the misfolded protein (Fá et al., 2016) that directly impinge on their function (Kaniyappan et al., 2017). Of note, many studies, including ours, in which synaptic and memory deficits were described in experimental models of tau accumulation in the brain (either transgenic mouse models of AD or WT mice subjected to intrahippocampal injection of tau) assessed the overall detrimental action of the misfolded protein accumulation without dissecting the relative contributions of astrocytes vs. neurons to the observed damage (Largo-Barrientos et al., 2021; Wu et al., 2021; Zhou et al., 2017). Therefore, we believe that data reported here strongly advance our understanding of the key role played by glial cells in the pathophysiology and spreading of the disease because of the synaptotoxic action caused by glial cells engulfment with tau oligomers (Briel et al., 2021; Hulshof et al., 2022; Perea et al., 2018; Piacentini et al., 2017; Richetin et al., 2020; Vogels et al., 2019; Wang et al., 2022).

We also found that ex-oTau entry in neural cells requires the expression of APP as demonstrated by the very poor oTau internalization in APP-KO neurons and astrocytes (Piacentini et al., 2017; Puzzo et al., 2017). The significantly lower synaptotoxic effects induced by 1-h ex-oTau application following pre-treatment with the anti-GPC4 antibody were similar to what we observed in APP KO cells/brain slices (Piacentini et al., 2017; Puzzo et al., 2017). Accordingly, APP KO cells/brain tissues had a significantly lower expression of GPC4 with respect to APP WT ones. Moreover, APP^{TA} mice in which threonine 668 was substituted with the non-phosphorylatable amino acid alanine, also showed very low levels of GPC4. This suggests that the expression of GPC4 receptor, mediating the entry and the synaptotoxic action of oTau, is regulated by the phosphor-Thr668-dependent, γ-secretase-mediated formation of the C-terminal domain of APP, AICD, that once translocated to the nucleus (Bukhari et al., 2017; Chang et al., 2006; Müller et al., 2008; von Rotz et al., 2004) has the potential to regulate the expression of the *Gpc4* gene. This hypothesis is fully supported by the results of our Ch-IP experiments showing AICD binding to the promoter of *Gpc4*.

Conclusions

Collectively, our study provides novel evidence on the crosstalk between APP cleavage and GPC4 expression playing a critical role in oTau accumulation in astrocytes. These phenomena underlie the astrocyte-dependent dysregulation of synaptic function significantly contributing to the pathophysiology of AD.

Supplementary Material

Refer to Web version on PubMed Central for supplementary material.

Acknowledgments

We would like to acknowledge the contribution of G-STeP Facilities (Electrophysiology and Microscopy) of Fondazione Policlinico Universitario “A. Gemelli” IRCCS for synaptic plasticity studies and confocal analyses.

Funding

This work was supported by Italian Ministry of Health, Ricerca Corrente 2023 - Fondazione Policlinico Universitario A. Gemelli IRCCS to C.G. and Università Cattolica del Sacro Cuore (D1 intramural funds) to R.P., as well as NIH-R01NS110024 to O.A.

List of abbreviations

Ex-oTau	extracellular tau oligomers
GPC4	glypican 4
HSPGs	Heparan Sulfate Proteoglycans
AID/AICD	Amyloid Precursor Protein Intracellular Domain
APP	Amyloid-beta precursor protein
LTP	long-term potentiation
GFAP	Glial fibrillary acidic protein

References

Allen NJ, Bennett ML, Foo LC, Wang GX, Chakraborty C, Smith SJ, Barres BA, 2012. Astrocyte glypicans 4 and 6 promote formation of excitatory synapses via GluA1 AMPA receptors. Nature 486, 410–414. 10.1038/nature11059 [PubMed: 22722203]

Aschenbrenner AJ, Gordon BA, Benzinger TLS, Morris JC, Hassenstab JJ, 2018. Influence of tau PET, amyloid PET, and hippocampal volume on cognition in Alzheimer disease. Neurology 91, e859–e866. 10.1212/WNL.0000000000006075 [PubMed: 30068637]

Briel N, Pratsch K, Roeber S, Arzberger T, Herms J, 2021. Contribution of the astrocytic tau pathology to synapse loss in progressive supranuclear palsy and corticobasal degeneration. Brain Pathology 31. 10.1111/bpa.12914

Bukhari H, Glotzbach A, Kolbe K, Leonhardt G, Loosse C, Müller T, 2017. Small things matter: Implications of APP intracellular domain AICD nuclear signaling in the progression and pathogenesis of Alzheimer’s disease. Prog Neurobiol 156, 189–213. 10.1016/j.pneurobio.2017.05.005 [PubMed: 28587768]

Chang K-A, Kim H-S, Ha T-Y, Ha J-W, Shin KY, Jeong YH, Lee J-P, Park C-H, Kim S, Baik T-K, Suh Y-H, 2006. Phosphorylation of Amyloid Precursor Protein (APP) at Thr668 Regulates the Nuclear Translocation of the APP Intracellular Domain and Induces Neurodegeneration. Mol Cell Biol 26, 4327–4338. 10.1128/MCB.02393-05 [PubMed: 16705182]

Condomitti G, de Wit J, 2018. Heparan Sulfate Proteoglycans as Emerging Players in Synaptic Specificity. Front Mol Neurosci 11. 10.3389/fnmol.2018.00014

de Wit J, O’Sullivan ML, Savas JN, Condomitti G, Caccese MC, Vennekens KM, Yates JR, Ghosh A, 2013. Unbiased Discovery of Glypican as a Receptor for LRRTM4 in Regulating Excitatory Synapse Development. Neuron 79, 696–711. 10.1016/j.neuron.2013.06.049 [PubMed: 23911103]

Fá M, Puzzo D, Piacentini R, Staniszewski A, Zhang H, Baltrons MA, Li Puma DD, Chatterjee I, Li J, Saeed F, Berman HL, Ripoli C, Gulisano W, Gonzalez J, Tian H, Costa JA, Lopez P, Davidowitz E, Yu WH, Haroutunian V, Brown LM, Palmeri A, Sigurdsson EM, Duff KE, Teich AF, Honig LS, Sierks M, Moe JG, D'Adamio L, Grassi C, Kanaan NM, Fraser PE, Arancio O, 2016. Extracellular Tau Oligomers Produce An Immediate Impairment of LTP and Memory. Sci Rep 6, 19393. 10.1038/srep19393 [PubMed: 26786552]

Farhy-Tselnicker I, van Casteren ACM, Lee A, Chang VT, Aricescu AR, Allen NJ, 2017. Astrocyte-Secreted Glypican 4 Regulates Release of Neuronal Pentraxin 1 from Axons to Induce Functional Synapse Formation. Neuron 96, 428–445.e13. 10.1016/j.neuron.2017.09.053 [PubMed: 29024665]

Guo JL, Lee VMY, 2014. Cell-to-cell transmission of pathogenic proteins in neurodegenerative diseases. Nat Med 20, 130–138. 10.1038/nm.3457 [PubMed: 24504409]

Guzman SJ, Gerevich Z, 2016. P2Y Receptors in Synaptic Transmission and Plasticity: Therapeutic Potential in Cognitive Dysfunction. Neural Plast 2016, 1–12. 10.1155/2016/1207393

Holmes BB, DeVos SL, Kfoury N, Li M, Jacks R, Yanamandra K, Ouidja MO, Brodsky FM, Marasa J, Bagchi DP, Kotzbauer PT, Miller TM, Papy-Garcia D, Diamond MI, 2013. Heparan sulfate proteoglycans mediate internalization and propagation of specific proteopathic seeds. Proceedings of the National Academy of Sciences 110. 10.1073/pnas.1301440110

Hulshof LA, van Nuijs D, Hol EM, Middeldorp J, 2022. The Role of Astrocytes in Synapse Loss in Alzheimer's Disease: A Systematic Review. Front Cell Neurosci 16. 10.3389/fncel.2022.899251

Kaniyappan S, Chandupatla RR, Mandelkow Eva-Maria, Mandelkow Eckhard, 2017. Extracellular low-n oligomers of tau cause selective synaptotoxicity without affecting cell viability. Alzheimer's & Dementia 13, 1270–1291. 10.1016/j.jalz.2017.04.002

Koizumi S, Fujishita K, Tsuda M, Shigemoto-Mogami Y, Inoue K, 2003. Dynamic inhibition of excitatory synaptic transmission by astrocyte-derived ATP in hippocampal cultures. Proceedings of the National Academy of Sciences 100, 11023–11028. 10.1073/pnas.1834448100

Kolay S, Vega AR, Dodd DA, Perez VA, Kashmer OM, White CL, Diamond MI, 2022. The dual fates of exogenous tau seeds: Lysosomal clearance versus cytoplasmic amplification. Journal of Biological Chemistry 298, 102014. 10.1016/j.jbc.2022.102014 [PubMed: 35525272]

Lagarde J, Olivieri P, Tonietto M, Tissot C, Rivals I, Gervais P, Caillé F, Moussion M, Bottlaender M, Sarazin M, 2022. Tau-PET imaging predicts cognitive decline and brain atrophy progression in early Alzheimer's disease. J Neurol Neurosurg Psychiatry 93, 459–467. 10.1136/jnnp-2021-328623 [PubMed: 35228270]

Lalo U, Palygin O, Verkhratsky A, Grant SGN, Pankratov Y, 2016. ATP from synaptic terminals and astrocytes regulates NMDA receptors and synaptic plasticity through PSD-95 multi-protein complex. Sci Rep 6, 33609. 10.1038/srep33609 [PubMed: 27640997]

Largo-Barrientos P, Apóstolo N, Creemers E, Callaerts-Vegh Z, Swerts J, Davies C, McInnes J, Wierda K, de Strooper B, Spires-Jones T, de Wit J, Uytterhoeven V, Verstreken P, 2021. Lowering Synaptogyrin-3 expression rescues Tau-induced memory defects and synaptic loss in the presence of microglial activation. Neuron 109, 767–777.e5. 10.1016/j.neuron.2020.12.016 [PubMed: 33472038]

Lasagna-Reeves CA, Castillo-Carranza DL, Sengupta U, Clos AL, Jackson GR, Kayed R, 2011. Tau oligomers impair memory and induce synaptic and mitochondrial dysfunction in wild-type mice. Mol Neurodegener 6, 39. 10.1186/1750-1326-6-39 [PubMed: 21645391]

Leone L, Colussi C, Gironi K, Longo V, Fusco S, Li Puma DD, D'Ascenzo M, Grassi C, 2019. Altered Nup153 Expression Impairs the Function of Cultured Hippocampal Neural Stem Cells Isolated from a Mouse Model of Alzheimer's Disease. Mol Neurobiol 56, 5934–5949. 10.1007/s12035-018-1466-1 [PubMed: 30689197]

Li Puma DD, Marcocci ME, Lazzarino G, de Chiara G, Tavazzi B, Palamara AT, Piacentini R, Grassi C, 2021. Ca^{2+} -dependent release of ATP from astrocytes affects herpes simplex virus type 1 infection of neurons. Glia 69, 201–215. 10.1002/glia.23895 [PubMed: 32818313]

Li Puma DD, Piacentini R, Leone L, Gironi K, Marcocci ME, de Chiara G, Palamara AT, Grassi C, 2019. Herpes Simplex Virus Type-1 Infection Impairs Adult Hippocampal Neurogenesis via Amyloid-β Protein Accumulation. Stem Cells 37, 1467–1480. 10.1002/stem.3072 [PubMed: 31381841]

Li Puma DD, Ripoli C, Puliatti G, Pastore F, Lazzarino G, Tavazzi B, Arancio O, Piacentini R, Grassi C, 2022. Extracellular tau oligomers affect extracellular glutamate handling by astrocytes through downregulation of GLT-1 expression and impairment of NKA1A2 function. Neuropathol Appl Neurobiol 48. 10.1111/nan.12811

Lombino F, Biundo F, Tamayev R, Arancio O, D'Adamio L, 2013. An Intracellular Threonine of Amyloid-β Precursor Protein Mediates Synaptic Plasticity Deficits and Memory Loss. PLoS One 8, e57120. 10.1371/journal.pone.0057120 [PubMed: 23451158]

Ma K, Xing S, Luan Y, Zhang C, Liu Yingfei, Fei Y, Zhang Z, Liu Yong, Chen X, 2021. Glypican 4 Regulates Aβ Internalization in Neural Stem Cells Partly via Low-Density Lipoprotein Receptor-Related Protein 1. Front Cell Neurosci 15. 10.3389/fncel.2021.732429

Mah D, Zhao J, Liu X, Zhang F, Liu J, Wang L, Linhardt R, Wang C, 2021. The Sulfation Code of Tauopathies: Heparan Sulfate Proteoglycans in the Prion Like Spread of Tau Pathology. Front Mol Biosci 8. 10.3389/fmolb.2021.671458

Marcatti M, Fracassi A, Montalbano M, Natarajan C, Krishnan B, Kayed R, Taglialatela G, 2022. Aβ/tau oligomer interplay at human synapses supports shifting therapeutic targets for Alzheimer's disease. Cellular and Molecular Life Sciences 79, 222. 10.1007/s00018-022-04255-9 [PubMed: 35377002]

Mecca AP, Chen M-K, O'Dell RS, Naganawa M, Toyonaga T, Godek TA, Harris JE, Bartlett HH, Zhao W, Banks ER, Ni GS, Rogers K, Gallezot JD, Ropchan J, Emery PR, Nabulsi NB, vander Wyk BC, Arnsten AFT, Huang Y, Carson RE, van Dyck CH, 2022. Association of entorhinal cortical tau deposition and hippocampal synaptic density in older individuals with normal cognition and early Alzheimer's disease. Neurobiol Aging 111, 44–53. 10.1016/j.neurobiolaging.2021.11.004 [PubMed: 34963063]

Müller T, Meyer HE, Egensperger R, Marcus K, 2008. The amyloid precursor protein intracellular domain (AICD) as modulator of gene expression, apoptosis, and cytoskeletal dynamics—Relevance for Alzheimer's disease. Prog Neurobiol 85, 393–406. 10.1016/j.pneurobio.2008.05.002 [PubMed: 18603345]

Nazere K, Takahashi T, Hara N, Muguruma K, Nakamori M, Yamazaki Y, Morino H, Maruyama H, 2022. Amyloid Beta Is Internalized via Macropinocytosis, an HSPG- and Lipid Raft-Dependent and Rac1-Mediated Process. Front Mol Neurosci 15. 10.3389/fnmol.2022.804702

Passer B, Pellegrini L, Russo C, Siegel RM, Lenardo MJ, Schettini G, Bachmann M, Tabaton M, D'Adamio L, 2000. Generation of an Apoptotic Intracellular Peptide by γ-Secretase Cleavage of Alzheimer's Amyloid ß Protein Precursor. Journal of Alzheimer's Disease 2, 289–301. 10.3233/JAD-2000-23-408

Perea G, Araque A, 2010. GLIA modulates synaptic transmission. Brain Res Rev 63, 93–102. 10.1016/j.brainresrev.2009.10.005 [PubMed: 19896978]

Perea JR, Llorens-Martín M, Ávila J, Bolós M, 2018. The Role of Microglia in the Spread of Tau: Relevance for Tauopathies. Front Cell Neurosci 12. 10.3389/fncel.2018.00172

Piacentini R, Li Puma DD, Mainardi M, Lazzarino G, Tavazzi B, Arancio O, Grassi C, 2017. Reduced gliotransmitter release from astrocytes mediates tau-induced synaptic dysfunction in cultured hippocampal neurons. Glia 65, 1302–1316. 10.1002/glia.23163 [PubMed: 28519902]

Pontecorvo MJ, Devous MD, Kennedy I, Navitsky M, Lu M, Galante N, Salloway S, Doraiswamy PM, Southekal S, Arora AK, McGeehan A, Lim NC, Xiong H, Truocchio SP, Joshi AD, Shcherbinin S, Teske B, Fleisher AS, Mintun MA, 2019. A multicentre longitudinal study of flortaucipir (18F) in normal ageing, mild cognitive impairment and Alzheimer's disease dementia. Brain 142, 1723–1735. 10.1093/brain/awz090 [PubMed: 31009046]

Puzzo D, Piacentini R, Fá M, Gulisano W, Li Puma DD, Staniszewski A, Zhang H, Tropea MR, Cocco S, Palmeri A, Fraser P, D'Adamio L, Grassi C, Arancio O, 2017. LTP and memory impairment caused by extracellular Aβ and Tau oligomers is APP-dependent. Elife 6. 10.7554/eLife.26991

Rauch JN, Chen JJ, Sorum AW, Miller GM, Sharf T, See SK, Hsieh-Wilson LC, Kampmann M, Kosik KS, 2018. Tau Internalization is Regulated by 6-O Sulfation on Heparan Sulfate Proteoglycans (HSPGs). Sci Rep 8, 6382. 10.1038/s41598-018-24904-z [PubMed: 29686391]

Rauch JN, Luna G, Guzman E, Audouard M, Challis C, Sibih YE, Leshuk C, Hernandez I, Wegmann S, Hyman BT, Gradinaru V, Kampmann M, Kosik KS, 2020. LRP1 is a master regulator of tau uptake and spread. Nature 580, 381–385. 10.1038/s41586-020-2156-5 [PubMed: 32296178]

Renna P, Ripoli C, Dagliyan O, Pastore F, Rinaudo M, Re A, Paciello F, Grassi C, 2022. Engineering a switchable single-chain TEV protease to control protein maturation in living neurons. Bioeng Transl Med 7. 10.1002/btm2.10292

Richetin K, Steullet P, Pachoud M, Perbet R, Parietti E, Maheswaran M, Eddarkaoui S, Bégard S, Pythoud C, Rey M, Caillierez R, Q Do K, Halliez S, Bezzi P, Buée L, Leuba G, Colin M, Toni N, Déglon N, 2020. Tau accumulation in astrocytes of the dentate gyrus induces neuronal dysfunction and memory deficits in Alzheimer's disease. Nat Neurosci 23, 1567–1579. 10.1038/s41593-020-00728-x [PubMed: 33169029]

Saroja SR, Gorbachev K, Julia T, Goate AM, Pereira AC, 2022. Astrocyte-secreted glypican-4 drives APOE4-dependent tau hyperphosphorylation. Proceedings of the National Academy of Sciences 119. 10.1073/pnas.2108870119

Sarrazin S, Lamanna WC, Esko JD, 2011. Heparan Sulfate Proteoglycans. Cold Spring Harb Perspect Biol 3, a004952–a004952. 10.1101/cshperspect.a004952

Siano G, Falcicchia C, Origlia N, Cattaneo A, di Primio C, 2021. Non-Canonical Roles of Tau and Their Contribution to Synaptic Dysfunction. Int J Mol Sci 22, 10145. 10.3390/ijms221810145 [PubMed: 34576308]

Snow AD, Cummings JA, Lake T, 2021. The Unifying Hypothesis of Alzheimer's Disease: Heparan Sulfate Proteoglycans/Glycosaminoglycans Are Key as First Hypothesized Over 30 Years Ago. Front Aging Neurosci 13. 10.3389/fnagi.2021.710683

Song L, Oseid DE, Wells EA, Coaston T, Robinson AS, 2022. Heparan Sulfate Proteoglycans (HSPGs) Serve as the Mediator Between Monomeric Tau and Its Subsequent Intracellular ERK1/2 Pathway Activation. Journal of Molecular Neuroscience 72, 772–791. 10.1007/s12031-021-01943-2 [PubMed: 35040015]

Stopschinski BE, Holmes BB, Miller GM, Manon VA, Vaquer-Alicea J, Prueitt WL, Hsieh-Wilson LC, Diamond MI, 2018. Specific glycosaminoglycan chain length and sulfation patterns are required for cell uptake of tau versus α-synuclein and β-amyloid aggregates. Journal of Biological Chemistry 293, 10826–10840. 10.1074/jbc.RA117.000378 [PubMed: 29752409]

Tavazzi B, Lazzarino G, Leone P, Amorini AM, Bellia F, Janson CG, di Pietro V, Ceccarelli L, Donzelli S, Francis JS, Giardina B, 2005. Simultaneous high performance liquid chromatographic separation of purines, pyrimidines, N-acetylated amino acids, and dicarboxylic acids for the chemical diagnosis of inborn errors of metabolism. Clin Biochem 38, 997–1008. 10.1016/j.clinbiochem.2005.08.002 [PubMed: 16139832]

Vogels T, Murgoci A-N, Hromádka T, 2019. Intersection of pathological tau and microglia at the synapse. Acta Neuropathol Commun 7, 109. 10.1186/s40478-019-0754-y [PubMed: 31277708]

von Rotz RC, Kohli BM, Bosset J, Meier M, Suzuki T, Nitsch RM, Konietzko U, 2004. The APP intracellular domain forms nuclear multiprotein complexes and regulates the transcription of its own precursor. J Cell Sci 117, 4435–4448. 10.1242/jcs.01323 [PubMed: 15331662]

Wang C, Fan L, Khawaja RR, Liu B, Zhan L, Kodama L, Chin M, Li Y, Le D, Zhou Y, Condello C, Grinberg LT, Seeley WW, Miller BL, Mok S-A, Gestwicki JE, Cuervo AM, Luo W, Gan L, 2022. Microglial NF-κB drives tau spreading and toxicity in a mouse model of tauopathy. Nat Commun 13, 1969. 10.1038/s41467-022-29552-6 [PubMed: 35413950]

Wu M, Zhang M, Yin X, Chen K, Hu Z, Zhou Q, Cao X, Chen Z, Liu D, 2021. The role of pathological tau in synaptic dysfunction in Alzheimer's diseases. Transl Neurodegener 10, 45. 10.1186/s40035-021-00270-1 [PubMed: 34753506]

Xiong Y, Sun S, Teng S, Jin M, Zhou Z, 2018. Ca2+-Dependent and Ca2+-Independent ATP Release in Astrocytes. Front Mol Neurosci 11. 10.3389/fnmol.2018.00224

Zhao J, Wu H, Tang X, 2021. Tau internalization: A complex step in tau propagation. Ageing Res Rev 67, 101272. 10.1016/j.arr.2021.101272 [PubMed: 33571704]

Zhou L, McInnes J, Wierda K, Holt M, Herrmann AG, Jackson RJ, Wang Y-C, Swerts J, Beyens J, Miskiewicz K, Vilain S, Dewachter I, Moechars D, de Strooper B, Spires-Jones TL, de Wit J, Verstreken P, 2017. Tau association with synaptic vesicles causes presynaptic dysfunction. Nat Commun 8, 15295. 10.1038/ncomms15295 [PubMed: 28492240]

Highlights

- Extracellular tau oligomers need GPC4 to enter astrocytes
- GPC4-mediated oligomeric tau-upload affects synaptic function
- The expression of GPC4 depends on Amyloid Precursor Protein Intracellular Domain

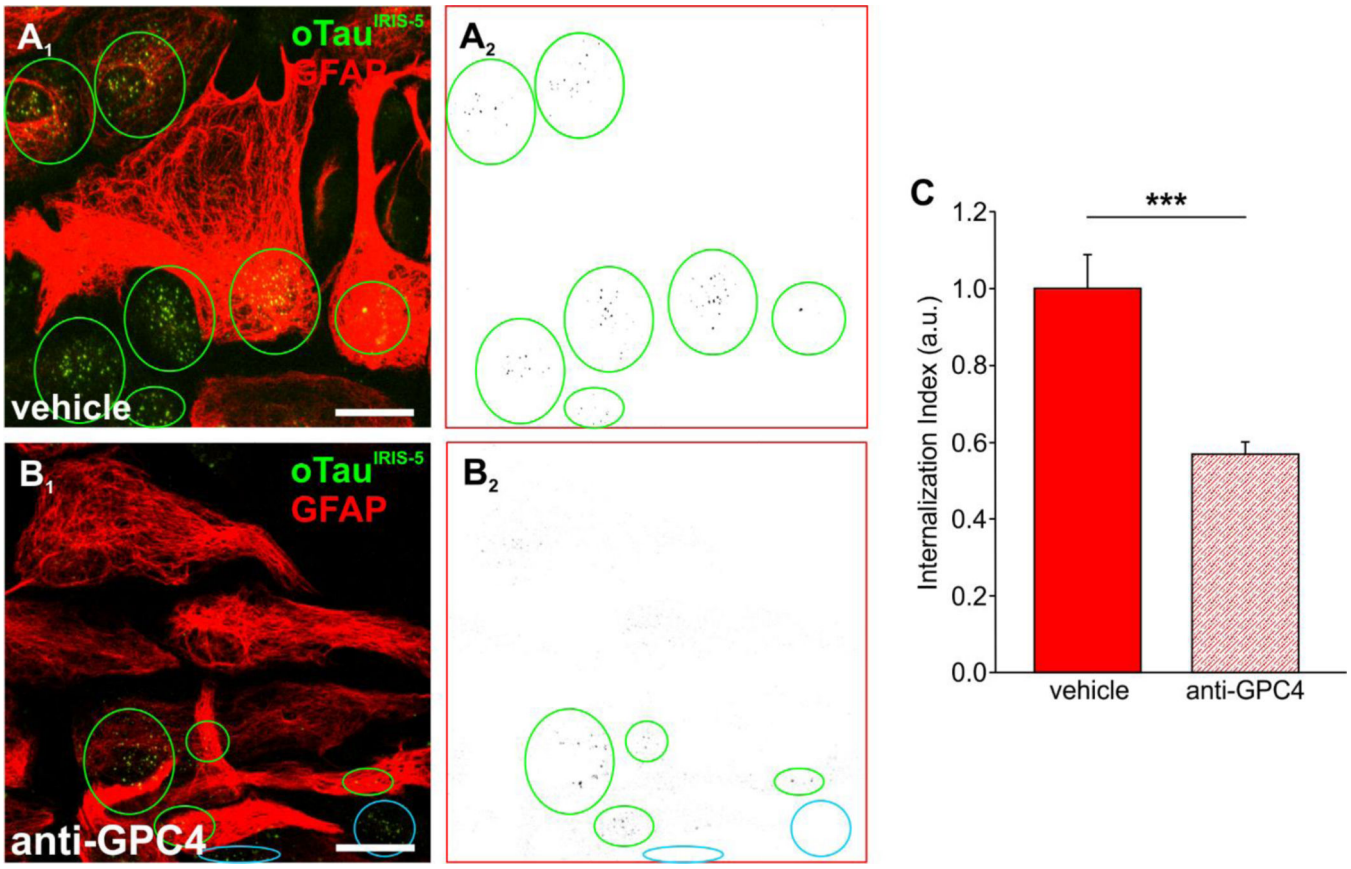

Figure 1. Treatment with anti-GPC4 antibody prevents ex-oTau internalization in astrocytes.

(**A_1**, **B_1**) Representative examples of oTau internalization in cultured hippocampal astrocytes treated for 24 hours with vehicle (A) or anti-GPC4 antibody (B) before 1-hour incubation with 200 nM ex-oTau in the culture medium. Tau oligomers were labelled with the IRIS-5 fluorophore ($oTau^{IRIS-5}$). (**A_2**, **B_2**) Panels showing the "internalization maps", where the black dots represent points in which the fluorescence of GFAP and $oTau^{IRIS-5}$ co-localizes, thus indicating oTau internalization. Ellipses in panels A and B indicate clusters of tau oligomers that i) are internalized (green) or (ii) remained attached to the plasma membrane of astrocytes without enter (blue). The presence of green dots in panel B_1 ($oTau^{IRIS-5}$-GFAP) that are not paralleled by black dots in the corresponding internalization map (panel B_2) indicate tau oligomers that are attached to the membrane but not (yet) internalized. Scale bars: 10 μm in A_1-B_1. **(C)** Bar graph showing Internalization Index (see Piacentini et al., 2017) for oTau, after 1-h incubation in the presence of vehicle, or 24-h pretreatment with anti GPC4. (n=10 independent fields by three independent experiments for both conditions). ***$p<0.001$.

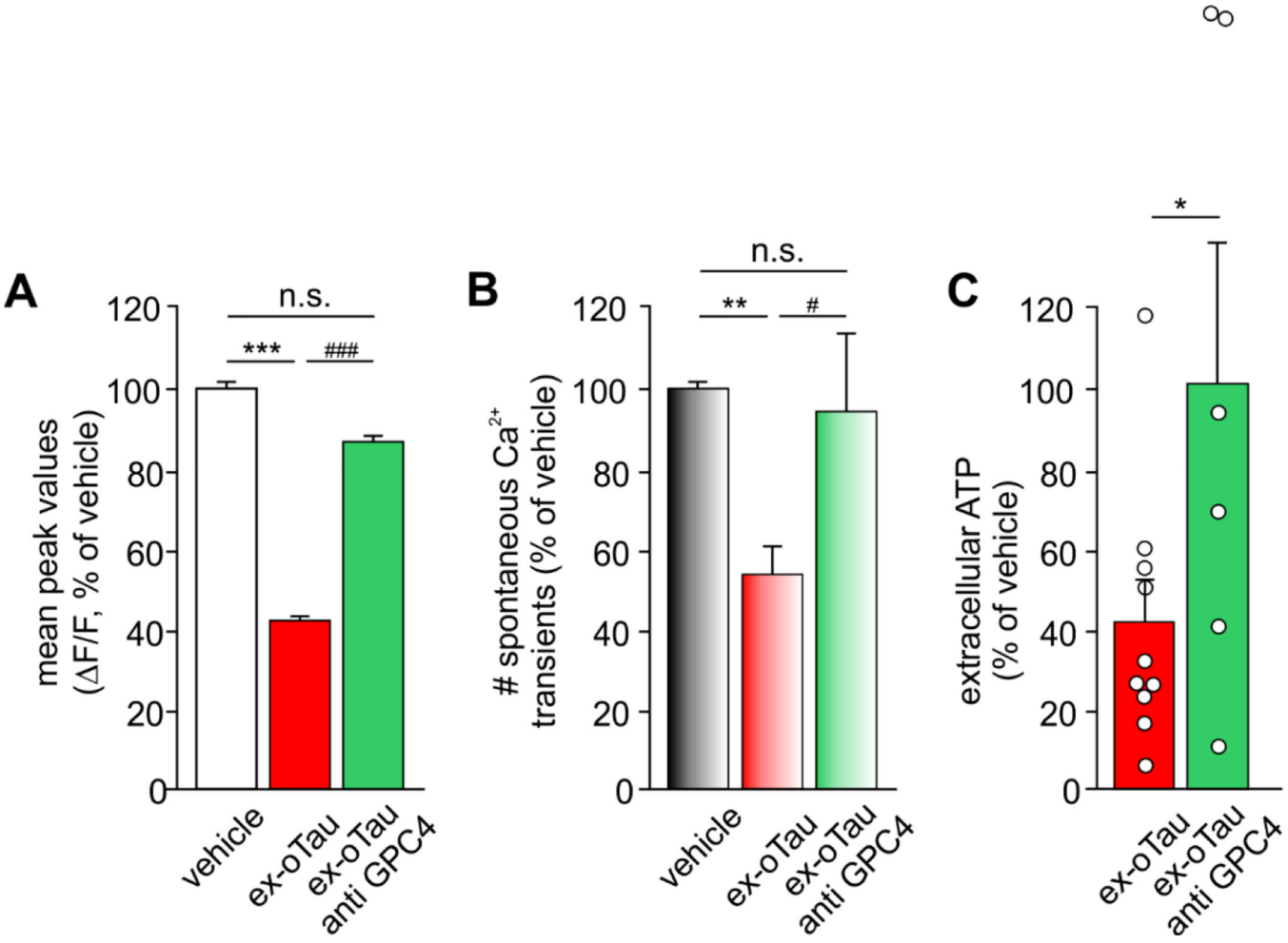

Figure 2. Treatment with anti-GPC4 antibody prevents ex-oTau-induced alteration of intracellular calcium signaling in astrocytes and restores gliotransmitter release from oTau-targeted astrocytes.

(A) Bar graphs showing the mean amplitude at peak (filled bars, left) of ATP (10 s, 100 μM)-induced intracellular Ca^{2+} transients in astrocytes treated for 1 hour with vehicle (n=254 studied cells) 200 nM ex-oTau (n=770) and ex-oTau after 24-h pretreatment with anti-GPC4 (n=570). **(B)** Faded bars show the mean number of spontaneous Ca^{2+} transients/min elicited after ATP stimulation in the above-mentioned conditions. **(C)** Bar graph showing the amount of ATP released by astrocytes in the culture medium in the following conditions: 1-h application of extracellular oligomeric tau after (n=6 independent experiments), or not (n=10), 24-h anti-GPC4 treatment. *p<0.05; **p<0.01; ***p<0.001; #p<0.05 and ###p<0.001.

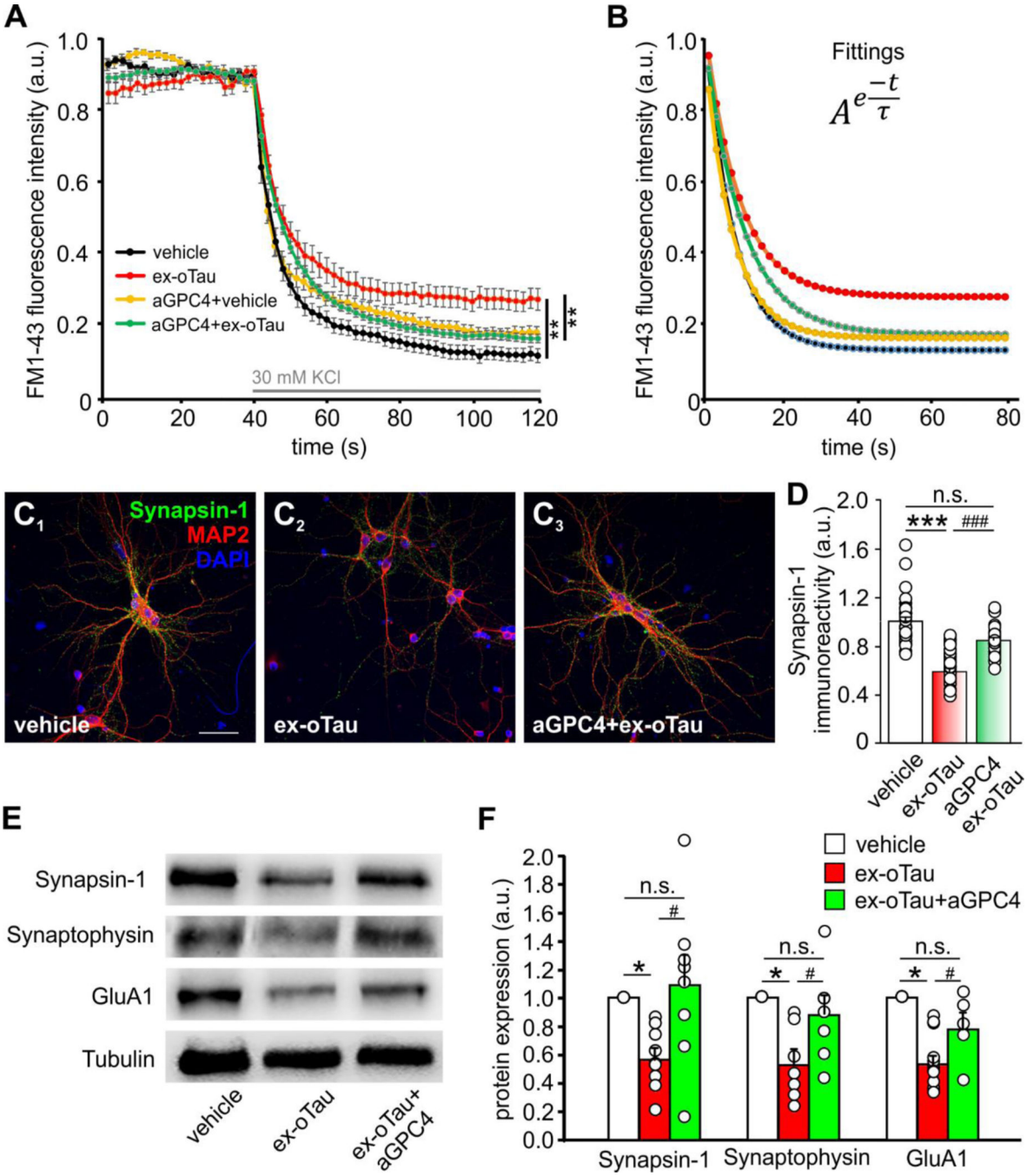

Figure 3. Treatment with anti-GPC4 antibody prevents ex-oTau-induced impairment of synaptic vesicle release and synaptic protein expression in hippocampal neurons.

(A) Mean time course of FM1–43 intensity following 30 mM KCl stimulation in hippocampal neurons co-cultured with astrocytes and treated for 1 hour with either vehicle or ex-oTau (200 nM) after 24-h pre-treatment with vehicle or anti-GPC4 (aGPC4). **(B)** Curves obtained by the fitting of the main curves in A with the equation used to evaluate the single parameters (A and τ) for each studied condition. n=28 neurons analyzed for vehicle/vehicle; n=18 for vehicle/ex-oTau; n=29 for vehicle/aGPC4; n=61 for aGPC4/ex-oTau.

(**$C_{1–3}$**) Representative confocal images of immunoreactivity of cultured murine hippocampal neurons (MAP2-positive) for Synapsin-1 in the following conditions: vehicle-treated, 1-h ex-oTau treatment, 1-h ex-oTau treatment following 24 h lasting cell incubation with anti-GPC4. DAPI was used to label cell nuclei. Scale bar: 10 μm. **(D)** Bar graph quantifying data of experiments represented in $C_{1–3}$. **(E)** Representative Western blot analysis carried-out on lysates from organotypic hippocampal slices treated as in panels $C_{1–3}$. **(F)** Bar graph showing densitometric analysis of experiments reported in panel E. *$p<0.05$ and ***$p<0.001$; # $p<0.05$ and ###$p<0.001$. n.s., not significant difference.

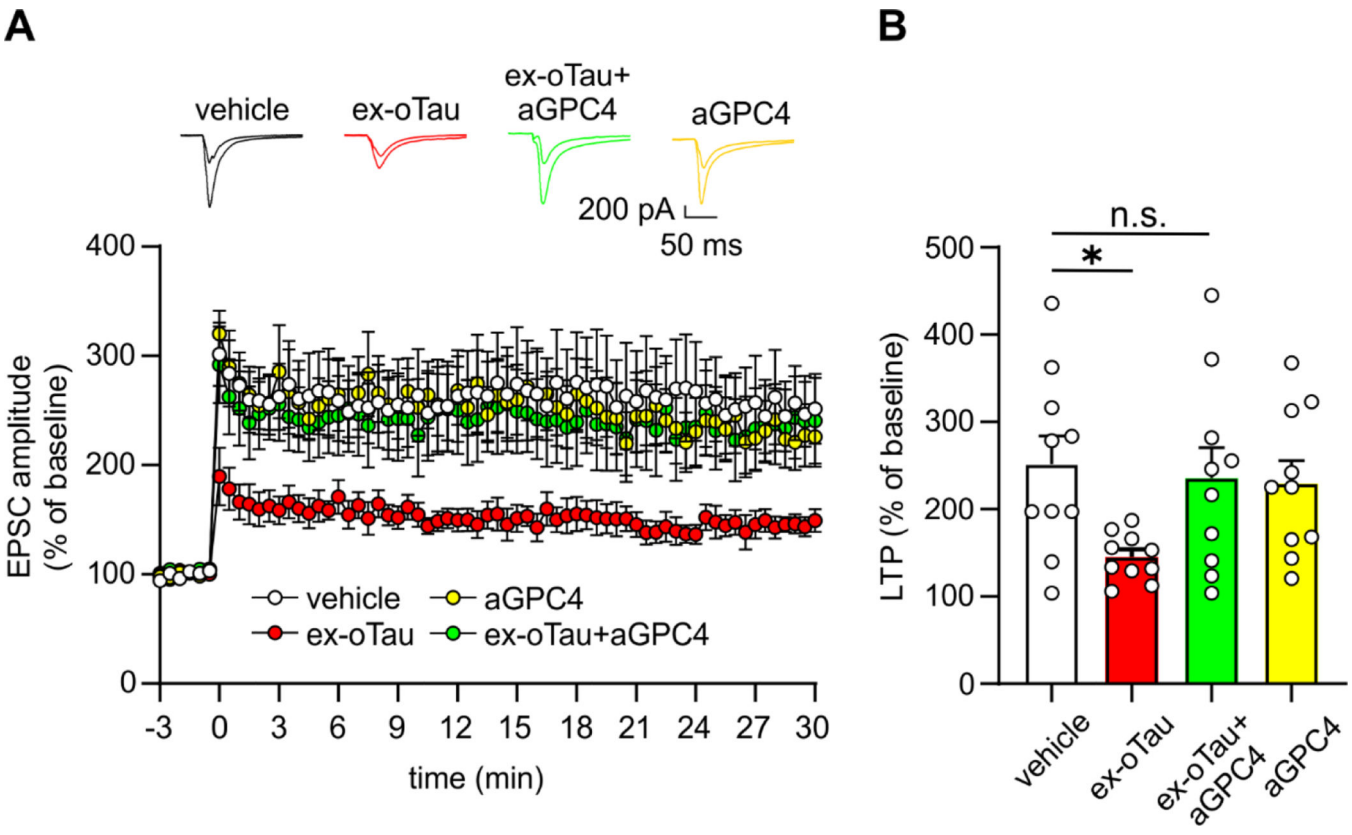

Figure 4. Treatment with anti-GPC4 antibody prevents ex-oTau-induced impairment of LTP at CA3-CA1 synapse in organotypic hippocampal slices.

(A) Time-course of excitatory post-synaptic currents (EPSCs) recorded in organotypic hippocampal slices at CA1 after pairing stimuli to CA3. Curves represent EPSCs in slices treated with vehicle (black dots; n=10), 1-h ex-oTau (200 nM) alone (red dots; n=10) or after 24-h incubation with anti-GPC4 (green dots; n=10). Treatment with antibody alone is shown in yellow (n=10). Slices were obtained from 3 independent preparations (4 mice/preparation). **(B)** Bar graph indicating the mean values of LTP evaluated in the last 5 min of EPSC recording, *$p<0.05$; n.s.: not significant difference.

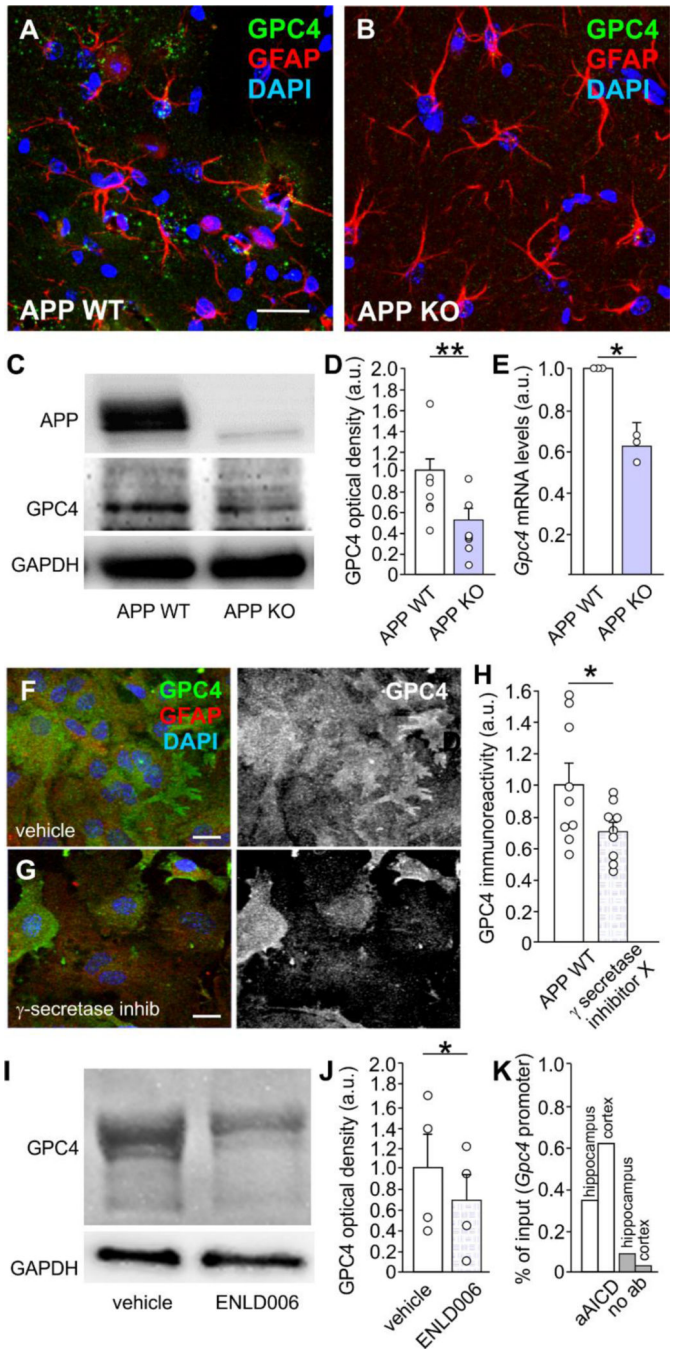

Figure 5. GPC4 expression depends on APP processing and AICD formation.

(A-B) Representative confocal images of a hippocampal section from WT (panel A) and APP KO (Panel B) immunolabeled for GFAP (red) and GPC4 (green). DAPI was used to stain cell nuclei. Scale bar 10 μm. **(C)** Representative Western blot analysis carried out on hippocampal lysates obtained from WT and APP KO mouse brain probed with anti GPC4 antibody (n=9 hippocampi for condition). **(D)** Bar graph quantifying the expression levels of GPC4 in experiments reported in panel C. **(E)** Bar graph showing relative expression of *Gpc4* mRNA evaluated in cultured astrocytes from WT and APP KO mice (n=3 independent

experiments for both). **(F-G)** Representative confocal images of GPC4 immunoreactivity in cultured astrocytes treated for 48 hours with vehicle (DMSO) or the γ secretase inhibitor X. Panels on the right represents GPC4 immunoreactivity only in the two conditions analyzed. Scale bar 10 μm. **(H)** Bar graph quantifying the expression levels of GPC4 in experiments reported in panel E-F. **(I)** Representative Western blot analysis carried out on lysated of cultured WT astrocytes treated for 48 hours with the inhibitor of the γ secretase ENLD006. **(J)** Bar graph quantifying the expression levels of GPC4 in experiments reported in panel I. **(K)** Bar graph showing the results of ChIP experiments demonstrating the binding of AICD to the *Gpc4* promoter (aAICD: antibody anti-AICD; no ab: no antibody). *p<0.05.

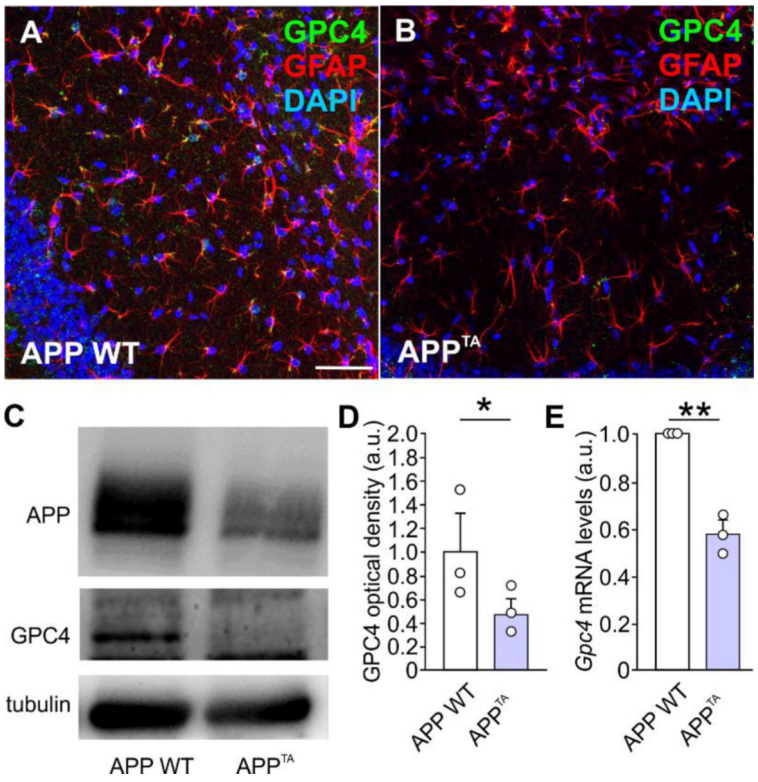

Figure 6. GPC4 expression depends on phosphorylation of APP at Thr668.

(A-B) Representative confocal images of hippocampal section from WT mice (panel A) and the APP^{TA} transgenic mice in which Threonine 668 of APP was substituted with non-phosphorylatable Alanine (Panel B), immunolabeled for GFAP (red) and GPC4 (green). DAPI was used to stain cell nuclei. Scale bar 75 μm. **(C)** Representative Western blot analysis carried out on hippocampal lysates obtained from WT and APP^{TA} mice probed with anti GPC4 antibody (n=3 independent experiments). **(D)** Bar graph quantifying the expression levels of GPC4 in experiments reported in panel C (n=3 independent experiments). **(E)** Bar graph showing relative expression of *Gpc4* mRNA evaluated in cultured astrocytes from WT and APP^{TA} mice (n=3 independent experiments for both). *p<0.05.